Materials Advances

ROYAL SOCIETY OF CHEMISTRY

COMMUNICATION

View Article Online
View Journal | View Issue

Cite this: *Mater. Adv.*, 2022, 3, 4155

Received 23rd March 2022,
Accepted 13th April 2022

DOI: 10.1039/d2ma00338d

rsc.li/materials-advances

Controlling coefficients of thermal expansion in thermoplastic materials: effects of zinc cyanide and ionic liquid†

Savannah Egerton,‡[a] Claudia Sim,‡[a] Heon E. Park,‡[a] Mark P. Staiger,[b] Komal M. Patil[c] and Matthew G. Cowan*[ac]

Tuning the coefficients of thermal expansion (CTE) of materials is necessary to control performance and extend the operational life of precision equipment. Herein, we report the strategy of creating 3-component composite materials from the thermoplastic poly(ethylene), zinc cyanide as a solid with a negative coefficient of thermal expansion (NTE), and ionic liquid 1-ethyl-3-methylimidazolium bis(trifluoromethylsulfonyl)imide ([EMIM][TFSI]) as an interfacial agent that enhances the polymer/solid interface. Specifically, we produce thermoplastic composites with coefficients of thermal expansion reduced from 290 to 190 $\times$ 10^{-6} K^{-1}, a significantly larger reduction than the *ca.* -15 $\times$ 10^{-6} K^{-1} reported for composites containing other NTE fillers. Additionally, the composite materials retain a Young's modulus comparable to low density polyethylene (80–110 MPa). Overall, this three-component design strategy shows promise for the development of thermoplastic materials with controlled coefficients of thermal expansion.

The coefficient of thermal expansion (CTE, α) describes a materials change in length in response to temperature. In electronic and mechanical devices, matching the CTE of components ensures the robustness, reliability and longevity of devices by reduces the likelihood of internal residual stresses developing due to temperature cycling.[1–5] In contrast, mismatch of components CTE can compromise the strength and integrity of the device components,[4,6,7] causing changes in temperature to render devices inoperable, particularly in electronics and high-precision applications.[8–13] Strategies for designing materials with tailored CTE are therefore particularly advantageous for applications in electronic systems[14–16] and optics,[3,7,17,18] and seals (*e.g.* O-rings, gaskets).[5,19]

While most materials exhibit a positive CTE, some materials contract with increasing temperature and display a negative coefficient of thermal expansion (NTE). Well-known examples include highly orientated aromatic polyamides,[20] graphite and graphene,[21] metal oxides (*e.g.* $PbTiO_3$,[22] ZrW_2O_8[23]), and metal–organic frameworks (*e.g.* zinc cyanide ($Zn(CN)_2$)).[24] $Zn(CN)_2$ is known to have a relatively large NTE, ranging from -19.8 $\times$ 10^{-6} K^{-1} at <180 K to -14 $\times$ 10^{-6} K^{-1} at >400 K.[3,8,9,25–27] The large NTE of $Zn(CN)_2$ is due to the vibrational modes of the metal–ligand bonds that cause transverse vibrational displacement of the zinc ions, resulting in a decrease in the distance between adjacent Zn ions.[8–10,28–31] The large NTE of $Zn(CN)_2$ makes it an interesting material for forming composites with controlled CTE.

The CTE of materials can be manipulated through chemical treatments[1,32–35] and compositional changes (*e.g.* fillers such as SiO_2).[36] To achieve a certain CTE, composite materials can incorporate a filler (or reinforcing) material with NTE.[6,37] Examples include orientated aromatic polyamides or graphite fibers to create polymer matrix composites with a low (or near-zero) CTE.[11,34] Recently, ZrW_2O_8 (NTE = -3 to -5 $\times$ 10^{-6} K^{-1}) has been combined with epoxy,[18] polyimide,[23] and cement to reduce the CTE of polymer and bonding materials.[3,7,19,37,38]

The nature of the filler–matrix interface in these composite systems is poorly understood. However, as demonstrated by Shubin *et al.*, the filler–matrix interfacial bonding (or incompatibility) will strongly influence both the overall CTE and mechanical properties of the resulting composite.[19] This occurs *via* phase separation, lack of adhesion, and formation of void space defects at the filler–matrix interface, which reduces the toughness and strength of the composite by nucleating crack formation and initiating other failure mechanisms.[5,19,39–41]

Attempts to improve filler–matrix interfacial adhesion include the addition of linker molecules (aka compatibilizers) that permit chemical bonding between the filler and polymer

[a] *Department of Chemical and Process Engineering, University of Canterbury, Christchurch, 8140, New Zealand. E-mail: matthew.cowan@canterbury.ac.nz*
[b] *Department of Mechanical Engineering, University of Canterbury, Christchurch, 8140, New Zealand*
[c] *MacDiarmid Institute for Advanced Materials and Nanotechnology, School of Physical and Chemical Sciences, University of Canterbury, Private Bag 4800, Christchurch, New Zealand*

† Electronic supplementary information (ESI) available. See DOI: https://doi.org/10.1039/d2ma00338d

‡ These authors contributed equally to this work.

matrix.[39] Alternatively, surface modification of the ZrW_2O_8 is used to enhance interfacial bonding with the matrix, thereby reducing the presence of voids.[38]

Interfacial defects also play a key role in the field of mixed-matrix membrane materials. There, the incorporation of ionic liquids (ILs) such as 1-ethyl-3-methylimidazolium bis(trifluoromethylsulfonyl) imide ([EMIM][TFSI]) has been reported to fill gas-transport defects at inorganic–organic interfaces improving selectivity and mechanical properties.[42–45]

Herein, we apply the strategy of ionic liquid and NTE filler incorporation to reduce the CTE of thermoplastic materials similar to those used in many electronic devices. Specifically, we demonstrate that [EMIM][TFSI] acts as an interfacial agent for eliminating interfacial defects in $Zn(CN)_2$-filled low density polyethylene composites, allowing control over the CTE and mechanical properties.

The composite materials were prepared by melt-casting of the thermoplastic low density poly(ethylene) (LDPE), NTE filler $Zn(CN)_2$, and ionic liquid [EMIM][TFSI]. Addition of $Zn(CN)_2$ produced increasingly brittle composite materials, and composites containing $>$ 40 wt. % $Zn(CN)_2$ could not be removed from the mould without fracturing, which set an upper limit on the $Zn(CN)_2$ content.

[EMIM][TFSI] was selected as the ionic liquid component due to its use studies on mixed-matrix membranes[42–45] and because it contains both polar (ionic) and non-polar functionality ($[TFSI]^-$ anion), that make it a suitable interfacial agent for the $Zn(CN)_2$ (polar) and LDPE (non-polar) interface. Interestingly, LDPE that contained [EMIM][TFSI], but no $Zn(CN)_2$, produced phase-separated materials with separated ionic liquid pockets. Thus, the C-0-X (refers to: Composite (C) with 0 wt% $Zn(CN)_2$ and x wt% [EMIM][TFSI]) samples were unsuitable for testing. In contrast, phase separation was not observed in composite formulations that contained both $Zn(CN)_2$ and IL. This implies that [EMIM][TFSI] interacts with the polar $Zn(CN)_2$ surface and therefore concentrates at the interface. The phase separation of [EMIM][TFSI] with neat LDPE suggests that future studies using ionic liquids more compatible with the LDPE matrix (*e.g.* longer aliphatic chains) may further enhance the interfacial adhesion at the polymer/NTE filler interface.

Scanning electron microscopy (SEM) images of the extreme cases of 40 wt% $Zn(CN)_2$ and no [EMIM][TFSI] (C-40-0) or 10 wt% [EMIM][TFSI] (C-40-10) reveal that [EMIM][TFSI] plays a significant role in combining the polymer with the $Zn(CN)_2$ (Fig. 1). All SEM images indicate that the composites are well-mixed with good dispersion of $Zn(CN)_2$ and no stratification or settling of the solid material within the polymer matrix occurred during preparation. The defined edges of $Zn(CN)_2$ in SEM images of (C-40-0) indicate that $Zn(CN)_2$ is poorly adhered to the polymer matrix. In contrast, SEM images of (C-40-10) show that the polymer has fully and intimately coated the $Zn(CN)_2$ particles. The rounded surfaces suggest good adherence has occurred at the interface.

Powder X-ray diffraction (PXRD) results (Fig. S2, ESI†) confirm that the crystal structure of $Zn(CN)_2$ was maintained during preparation of the composites. Zinc and iron cyanide

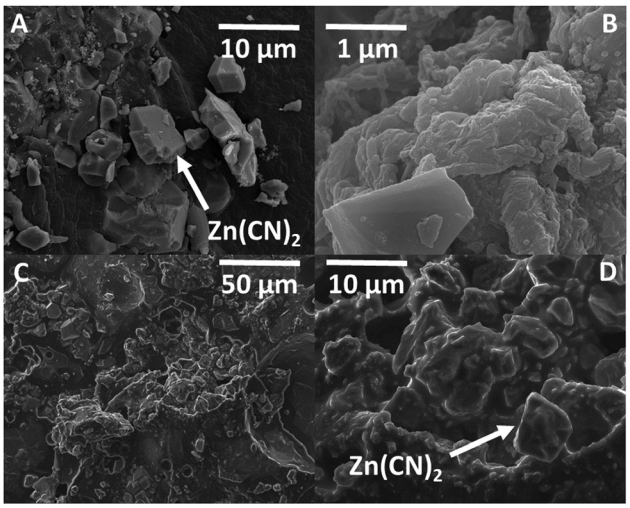

Fig. 1 SEM images of the LDPE/$Zn(CN)_2$ interfaces on the fracture surfaces of composites (A) (C-40-0), (B) (C-20-2.5), (C) (C-40-10), and (D) (C-40-10). Note the superior integration of the $Zn(CN)_2$ crystallites into the LDPE matrix, indicated by rounded edges, when an sufficient amount of ionic liquid is present.

complexes are known to be insoluble in imidazolium ionic liquids.[46]

The moisture content and decomposition behaviour of the composites were measured using TGA to ensure that the materials were not hygroscopic and that exposure to ambient humidity causing variation in residual water content would not affect testing. No mass loss corresponding to water evaporation is observed (Fig. S1, ESI†) suggesting that the hydrophobic nature of the polymer and [EMIM][TFSI] are sufficient to prevent water absorption. The onset of decomposition (T_d) of the composite occurs at $\sim$ 350 °C and the remaining residual mass corresponds to the amount of $Zn(CN)_2$ (T_d = 800 °C) within the composite.

The CTE of the composite materials were measured using thermomechanical analysis (TMA) (Fig. 2; Table 1). Addition of $Zn(CN)_2$ to the LDPE matrix decreased the coefficient of thermal expansion of the LDPE from 290 to 210 $\times$ 10^{-6} K^{-1} (The CTE values reported are average values for the range −40 °C to 80 °C). Incorporation of [EMIM][TFSI] content into the composites further *decreased* the CTE by *ca.* 20 $\times$ 10^{-6} K^{-1} (Fig. S4, ESI†). This result is in contrast to what is expected from a the law of mixtures (ESI,† Section 3), which predicts the addition of [EMIM][TFSI] (which has a positive CTE) to increase the overall CTE of the composites. This suggests that improving the LDPE/$Zn(CN)_2$ interface enhances the ability of an NTE filler to reduce the overall CTE of a composite, significantly expanding the range of CTE values accessible to thermoplastics such as LDPE.

In absolute terms, the addition of $Zn(CN)_2$ to LDPE decreased the CTE from 290 to 210 $\times$ 10^{-6} K^{-1} (Fig. 2; Table 1). The addition of 5 wt% [EMIM][TFSI] further decreases the CTE of the 40 wt% composite to 190 $\times$ 10^{-6} K^{-1} (ESI,† Section 3). The overall CTE decrease of 100 $\times$ 10^{-6} K^{-1} is *an order of magnitude higher* than the CTE reduction observed for

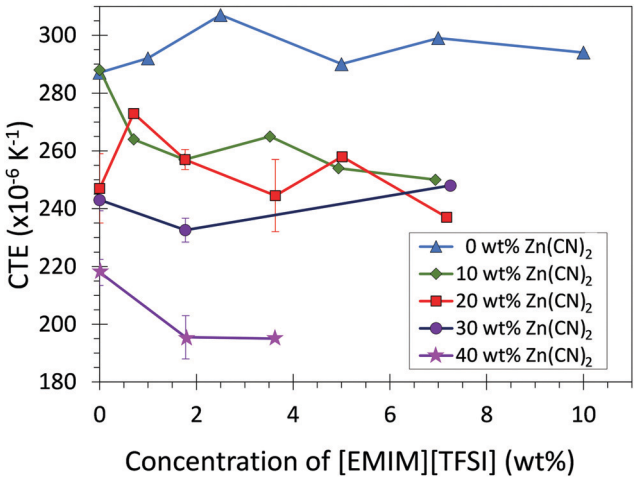

Fig. 2 CTE data measured for LDPE/Zn(CN)$_2$/[EMIM][TFSI] composites. Increasing the proportion of Zn(CN)$_2$ within the matrix results in a *ca.* 80 × 10^{-6} K^{-1} decrease of the CTE values. In contrast, the presence of [EMIM][TFSI] decreases the CTE of the composite by *ca.* 20 × 10^{-6} K^{-1}. The CTE values reported are average values for the range −40 °C to 80 °C. Lines are provided to guide the eye. Error bars represent the standard deviation of measurements on replicate samples.

Table 1 CTE data measured for LDPE/Zn(CN)$_2$/[EMIM][TFSI] composites compared to composites reported in the literature. CTE values of neat material

Material	CTE (10^{-6} K^{-1})
LDPE	291
Zn(CN)$_2$	−19.8 to −14[8]
[EMIM][TFSI]	649
0 wt% Zn(CN)$_2$/LDPE	290
40 wt% Zn(CN)$_2$/LDPE	210
0 wt% Zn(CN)$_2$/LDPE/5 wt% [EMIM][TFSI]	310
40 wt% Zn(CN)$_2$/LDPE/5 wt% [EMIM][TFSI]	190
$Zr_2WP_2O_{12}$	−3 to −5[38]
Polyimide	45[37]
40 wt. % ZWP/polyimide	30[7,23]

polyimide composites containing 40 wt% ZrW_2O_8 (15 × 10^{-6} K^{-1}) without the use of an interfacial agent.[7,47]

Addition of Zn(CN)$_2$ enhanced the stiffness (Young's modulus) of the materials due to the solid nature of Zn(CN)$_2$, while addition of [EMIM][TFSI] decreases the compliance due to the liquid nature of [EMIM][TFSI] (Fig. 3). Both toughness and tensile strength of the composites decreased with increasing amounts of Zn(CN)$_2$ and [EMIM][TFSI] due to a decrease in elongation at break (Fig. S6–S11, ESI†). Although less ductile with increasing amounts of Zn(CN)$_2$, the composite strength remains constant, especially encouraging for applications in devices where composites would not experience severe elongation.

In summary, we have developed a strategy for significantly reducing the CTE of thermoplastic composite materials and applied it to the production of LDPE composites with Zn(CN)$_2$ fillers and ionic liquid interfacial agents. The reductions in CTE are an order of magnitude higher than reported from previous materials, allowing reduction of the neat polymer CTE by

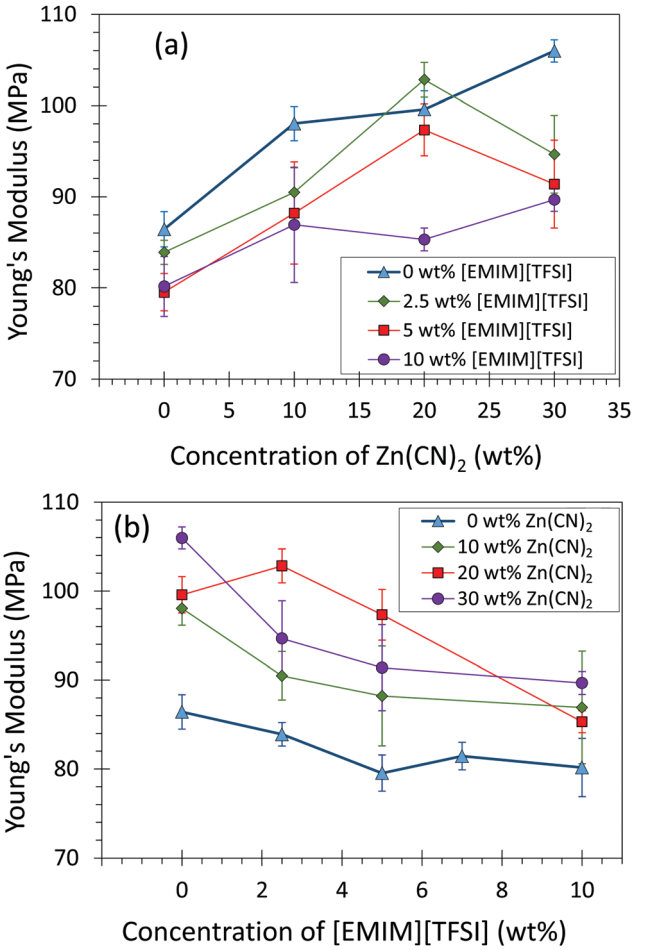

Fig. 3 Young's modulus for LDPE/Zn(CN)$_2$/[EMIM][TFSI] composites. (a) Young's modulus slightly increases with the concentration of Zn(CN)$_2$, (b) that slightly decreases with [EMIM][TFSI]. Lines are provided to guide the eye. Error bars represent the standard deviation of measurements on replicate samples.

up to −80 × 10^{-6} K^{-1}. Furthermore, inclusion of ionic liquid as an interfacial agent results in retention of tensile strength similar to neat LDPE. We anticipate the strategy of combining polymers with NTE fillers and ionic liquids will be useful for producing thermoplastic materials with controlled coefficients for use in precision electronic and mechanical devices.

Conflicts of interest

There are no conflicts to declare.

Acknowledgements

We thank the MacDiarmid Institute for supporting a Research Associate position for Savannah Egerton.

References

1 J. Chen, L. Hu, J. Deng and X. Xing, *Chem. Soc. Rev.*, 2015, **44**, 3522–3567.

2 R. C. Wetherhold and J. Wang, *Compos. Sci. Technol.*, 1995, **53**, 1–6.
3 J. Shi, Z. Pu, K. H. Wu and G. Larkins, *MRS Online Proc. Libr.*, 1996, **445**, 229–234.
4 E. Della Gaspera, R. Tucker, K. Star, E. H. Lan, Y. S. Ju and B. Dunn, *ACS Appl. Mater. Interfaces*, 2013, **5**, 10966–10974.
5 K. Takenaka, K. Kuzuoka and N. Sugimoto, *J. Appl. Phys.*, 2015, **118**, 084902.
6 R. Huang, Z. Chen, X. Chu, Z. Wu and L. Li, *J. Compos. Mater.*, 2011, **45**, 1675–1682.
7 X. Shi, H. Lian, X. Yan, R. Qi, N. Yao and T. Li, *Mater. Chem. Phys.*, 2016, **179**, 72–79.
8 A. L. Goodwin and C. J. Kepert, *Phys. Rev. B: Condens. Matter Mater. Phys.*, 2005, **71**, 140301.
9 A. L. Goodwin, K. W. Chapman and C. J. Kepert, *J. Am. Chem. Soc.*, 2005, **127**, 17980–17981.
10 A. E. Phillips, G. J. Halder, K. W. Chapman, A. L. Goodwin and C. J. Kepert, *J. Am. Chem. Soc.*, 2010, **132**, 10–11.
11 K. Takenaka, T. Hamada, D. Kasugai and N. Sugimoto, *J. Appl. Phys.*, 2012, **112**, 083517.
12 K. Takenaka, *Front. Chem.*, 2018, 6.
13 L. Lei, L. Bolzoni and F. Yang, *Adv. Compos. Hybrid Mater.*, 2021, DOI: **10.1007/s42114-021-00248-7**.
14 J. Chen, Y. Zhu, X. Chang, D. Pan, G. Song, Z. Guo and N. Naik, *Adv. Funct. Mater.*, 2021, **31**, 2104686.
15 J. Chen, Y. Zhu, Z. Guo and A. G. Nasibulin, *Eng. Sci.*, 2020, **12**, 13–22.
16 N. Jiang, D. Hu, Y. Xu, J. Chen, X. Chang, Y. Zhu, Y. Li and Z. Guo, *Adv. Compos. Hybrid Mater.*, 2021, **4**, 574–583.
17 R. Roy, D. K. Agrawal and H. A. McKinstry, *Annu. Rev. Mater. Sci.*, 1989, **19**, 59–81.
18 P. Badrinarayanan, M. Rogalski, H. Wu, X. Wang, W. Yu and M. R. Kessler, *Macromol. Mater. Eng.*, 2013, **298**, 136–144.
19 S. Shubin, A. Akulichev and A. Freidin, *Mater. Phys. Mech.*, 2017, 32.
20 S. Rojstaczer, D. Cohn and G. Marom, *J. Mater. Sci. Lett.*, 1985, **4**, 1233–1236.
21 N. Mounet and N. Marzari, *Phys. Rev. B: Condens. Matter Mater. Phys.*, 2005, **71**, 205214.
22 A. Chandra, W. H. Meyer, A. Best, A. Hanewald and G. Wegner, *Macromol. Mater. Eng.*, 2007, **292**, 295–301.
23 J. Yang, Y. Yang, Q. Liu, G. Xu and X. Cheng, *J. Mater. Sci. Technol.*, 2010, **26**, 665–668.
24 D. J. Williams, D. E. Partin, F. J. Lincoln, J. Kouvetakis and M. O'Keeffe, *J. Solid State Chem.*, 1997, **134**, 164–169.
25 J. Zwanziger, *Phys. Rev. B: Condens. Matter Mater. Phys.*, 2007, **76**, 052102.
26 T. Ravindran, A. Arora, S. Chandra, M. Valsakumar and N. C. Shekar, *Phys. Rev. B: Condens. Matter Mater. Phys.*, 2007, **76**, 054302.
27 K. W. Chapman, P. J. Chupas and C. J. Kepert, *J. Am. Chem. Soc.*, 2005, **127**, 15630–15636.
28 K. W. Chapman and P. J. Chupas, *J. Am. Chem. Soc.*, 2007, **129**, 10090–10091.
29 J. O. Evans, *J. Chem. Soc., Dalton Trans.*, 1999, 3317–3326.
30 V. E. Fairbank, A. L. Thompson, R. I. Cooper and A. L. Goodwin, *Phys. Rev. B: Condens. Matter Mater. Phys.*, 2012, **86**, 104113.
31 J. Michael, W. Catherine and W. Mary, *J. Therm. Anal. Calorim.*, 2009, **99**, 165–172.
32 J. Chen, X. Xing, R. Yu and G. Liu, *J. Am. Ceram. Soc.*, 2005, **88**, 1356–1358.
33 C. Sun, Z. Cao, J. Chen, R. Yu, X. Sun, P. Hu, G. Liu and X. Xing, *Phys. Status Solidi B*, 2008, **245**, 2520–2523.
34 S. Wang, M. Tambraparni, J. Qiu, J. Tipton and D. Dean, *Macromolecules*, 2009, **42**, 5251–5255.
35 T.-C. Lim, *Adv. Compos. Hybrid Mater.*, 2021, **4**, 966–978.
36 X. Ye, B. Tian, Y. Guo, F. Fan and A. Cai, *Beilstein J. Nanotechnol.*, 2020, **11**, 671–677.
37 C. Lind, *Materials*, 2012, **5**, 1125–1154.
38 C. Lind, M. R. Coleman, L. C. Kozy and G. R. Sharma, *Phys. Status Solidi B*, 2011, **248**, 123–129.
39 L. M. Sullivan and C. M. Lukehart, *Chem. Mater.*, 2005, **17**, 2136–2141.
40 X. Chu, R. Huang, H. Yang, Z. Wu, J. Lu, Y. Zhou and L. Li, *Mater. Sci. Eng., A*, 2011, **528**, 3367–3374.
41 A. George, *Kirk-Othmer Encycl. Chem. Technol.*, 2000, 1–46.
42 Z. V. Singh, M. G. Cowan, W. M. McDanel, Y. Luo, R. Zhou, D. L. Gin and R. D. Noble, *J. Membr. Sci.*, 2016, **509**, 149–155.
43 Y. C. Hudiono, T. K. Carlisle, J. E. Bara, Y. Zhang, D. L. Gin and R. D. Noble, *J. Membr. Sci.*, 2010, **350**, 117–123.
44 Y. C. Hudiono, T. K. Carlisle, A. L. LaFrate, D. L. Gin and R. D. Noble, *J. Membr. Sci.*, 2011, **370**, 141–148.
45 G. H. Teoh, P. C. Tan, A. L. Ahmad and S. C. Low, *J. Membr. Sci. Res.*, 2021, **7**, 29–37.
46 J. Shi, Z. Shi, H. Yan, X. Wang, X. Zhang, Q. Lin and L. Zhu, *RSC Adv.*, 2018, **8**, 6565–6571.
47 C. Yang, J. Li, D. Yang, S. Li, Y. Qin, S. Meng and S. Du, *ACS Sustainable Chem. Eng.*, 2019, **7**, 14747–14755.